

PROCESSING AND BREAKDOWN LOCALIZATION RESULTS FOR AN L-BAND STANDING-WAVE CAVITY *

Faya Wang and Chris Adolphsen, SLAC, Menlo Park, CA 94025, U.S.A.

Abstract

An L-band (1.3 GHz), normal-conducting, 5-cell, standing-wave cavity that was built as a prototype capture accelerator for the ILC is being high-power processed at SLAC. The goal is to demonstrate stable operation of the cavity at more than 12 MV/m with 1 msec, 5 Hz pulses while it is immersed in a 0.5 T solenoidal magnetic field. This paper summarizes the performance that has been achieved and describes a novel analysis of the modal content of the stored energy in the cavity after a breakdown to determine the iris on which it occurred.

INTRODUCTION

A half-length (5-cell) prototype π -mode standing-wave cavity was built at SLAC to verify that the relatively high gradient (> 12 MV/m) required for efficient positron capture can be reliably achieved with the long (1.0 ms) ILC pulses [1 2 3]. Figure 1 shows a cross section of the cavity, whose design was complicated by the extensive cooling required to prevent significant detuning from average rf heating during its 5 Hz operation.

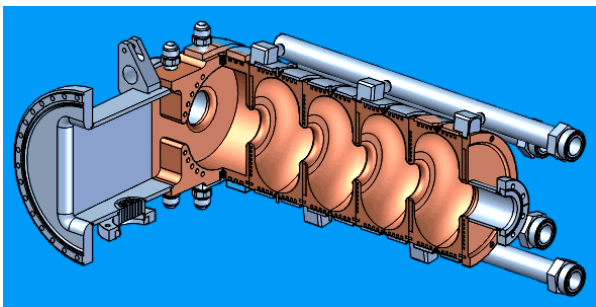
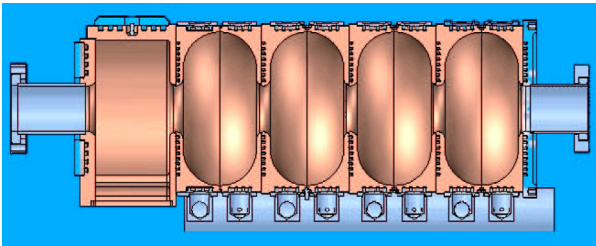


Figure 1: Cross sectional view of the 5-cell cavity where the coupler cell is on the left and an rf probe (not shown) is located in the beam pipe just outside the right-most cell. Cooling water circulates through rectangular grooves in the irises and outer cavity walls to remove up to 25 kW of average power.

At NLCTA, a single bunch of about 20 pC was accelerated at 5 Hz in the cavity at different injection

times (175 μ s and 610 μ s) during rf pulses with different widths (180 μ s and 1050 μ s). These combinations were chosen to distinguish the detuning effects from low average heating, high average heating and intra-pulse heating. The gradients inferred from the bunch energy gains are plotted in Fig 2 versus the net cavity input power. No significant gradient changes were observed for the different timing combinations, as was expected.

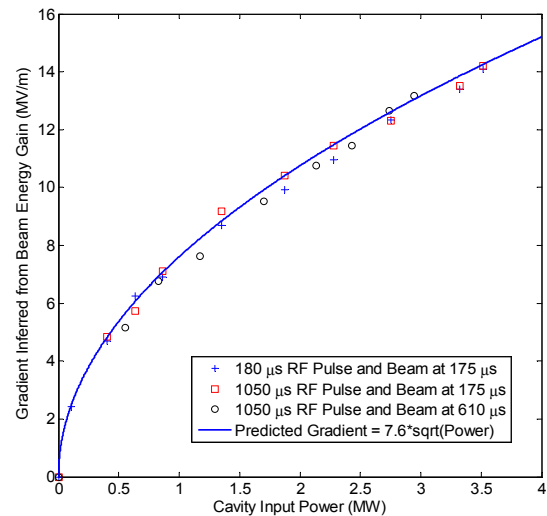


Figure 2: Predicted gradient and measured gradients versus the net cavity input power (forward minus reflected) for different pulse widths and bunch injection times.

The cavity has operated at 5 Hz with 1 ms pulses for about 1000 hours, mostly at the power-limited gradient of about 14 MV/m. The breakdown rate at this gradient is typically 1/hr whether or not the cavity is immersed in a 0.5 T solenoidal magnet as would be the case at ILC.

Although the cavity reached the design gradient, it incurred several thousand breakdowns during rf processing. Interestingly, the subsequent decay time of the stored energy after breakdown, which was measured with the downstream rf probe, varied greatly from event to event, taking from a few μ s to over 15 μ s to decrease by 20 dB. Also, there appeared to be a beating pattern in the waveform during the decays, all of which suggests that the breakdowns were causing the rf energy to be isolated in the downstream cells, and that the trapped energy was being partitioned among the resulting modes of those cells. This prompted a study of the cavity modes with an equivalent circuit model to see if the predicted decay spectra for various isolated downstream cells match the data spectra, thus identifying the likely irises on which the breakdowns had occurred.

* Work Supported by DOE Contract DE-AC03-76F00515.

BREAKDOWN LOCALIZATION

Measurements of ions emitted during breakdown in a 30 GHz structure show their maximum velocity to be about $1e4$ m/s [4]. If the velocities are similar in the ILC cavity, then the plasma generated by rf breakdown would spread out on the order of 1 cm in $1 \mu\text{s}$, which is small compared to the 10 cm iris spacing, but more significant compared to the 3 cm iris radius. So on this timescale, the largest plasma effect may be to reduce the coupling through the irises in which the breakdown occurs. This will be assumed in the following analysis, and is supported by other observations that are described below.

To simulate the effect of a breakdown on a particular iris with the equivalent circuit model, the cell-to-cell coupling through that iris was set to zero after the fields reached steady state in the π -mode. This model shows that the stored energy remaining in each section of the divided cavity will excite all possible modes in that section to some degree. As these modes decay, the amplitude of the store energy shows a beating pattern that depends on the frequency differences. Figure 3 shows plots of the Fourier Transform (FT) of the log of the simulated probe power (no phase information is used) in the downstream section during a $10 \mu\text{s}$ period after different irises are blocked. In the case where no irises are blocked, the initial field in the first cell was assumed to be 3 percent lower than the others to produce a noticeable beating. For the other cases, the initial fields in the cells were assumed to be equal, which may not be the case just after breakdown due to the loading caused by breakdown-generated currents.

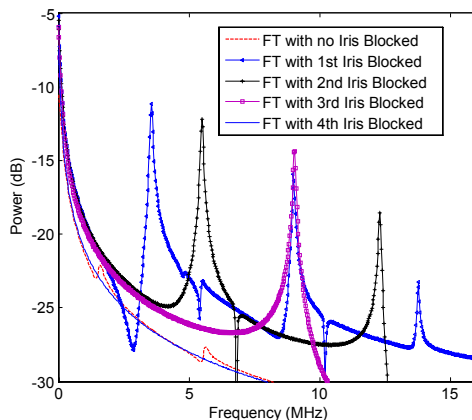


Figure 3: Predicted frequency spectrum of the log of the probe power at the downstream end of the cavity when different irises are blocked and the cell fields are equal initially, except for the no iris blocked case, in which the first cell has a field 3% lower than the others.

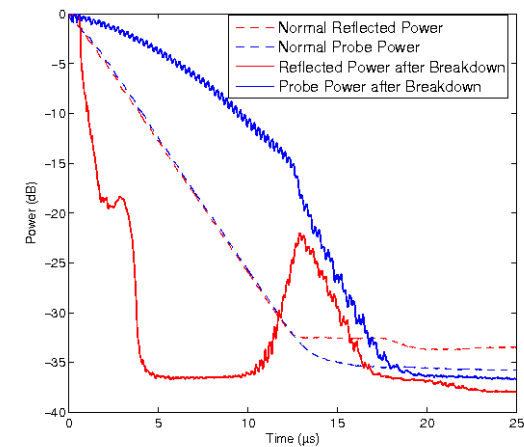
Figure 4a shows typical waveform data in the case where the breakdown appears to occur on the first of the four irises based on the analysis presented here. The data were taken with a 100 MHz sampling scope that started ($t = 0$) shortly after the main input power was shutoff (which occurred about $1 \mu\text{s}$ after a fault was detected).

Both the reflected and probe power are normalized to 0 dB at this point, as are these values for the non-breakdown event waveforms that are shown with dashed lines in the figure (in this case, the two curves track each other as expected for the critically coupled cavity). For the breakdown events, the reflected power decreases very fast, but has a profile that is complicated by the fact that the input power was first reduced by about 20 dB before $t = 0$ and then was fully shut off a few μs later through a different mechanism. Hence the ‘ledge’ in the reflected power curve at about -20 dB for a few μs before it falls to the measurement noise level at around -35 dB. In contrast, the probe power, which is a measure of stored energy, decreases relatively slowly, and shows that the breakdown was effective at isolating the downstream portion of the cavity. In fact, the probe power decay rate is about half the nominal rate (i.e., roughly consistent with Q_0) so the isolating mechanism does not itself absorb much power (although for the other iris cases, it does decrease faster).

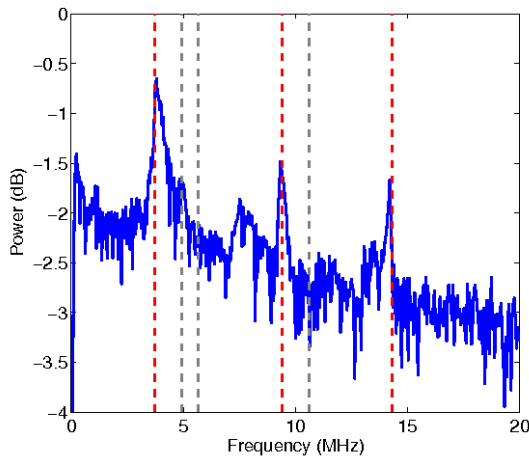
Another interesting feature of the data in Figure 4a is the eventual turn on the reflected power that then tracks the decay of the probe power after $t = 13 \mu\text{s}$. The mechanism that was isolating the stored energy appears to be no longer effective so the energy flows out through the coupler and appears as reflected power. The timescale for this transition is similar to that observed in X-band structures [5], and suggests the effect is a function of the plasma properties only (e.g., the recombination time of the ions and electrons).

Figure 4 also includes plots of the FT of the log of the probe power computed over the time ranges noted in the figure caption. The red-dashed vertical lines are those corresponding to the peaks in Figure 3 (in which it is assumed the isolated cells have equal fields initially), and the gray-dashed vertical lines are all possible additional beating frequencies. The good agreement of the data peaks with those in Figure 3 suggests the breakdown in this case is isolating the stored energy in the downstream four cells. However, it is not clear why the data peaks are less pronounced than in the simulations (and correspondingly, the simulated probe power signal has much higher peak-to-valley variations than the data). In Figure 4c, a similar FT comparison is made, but this time with the data after the reflected power turns on again. In this case, the vertical lines are for the full five cell cavity with the downstream four cells having equal fields initially and the coupler cell having zero field initially. The match of the vertical lines to the data peaks is consistent with the un-blocking of the first iris.

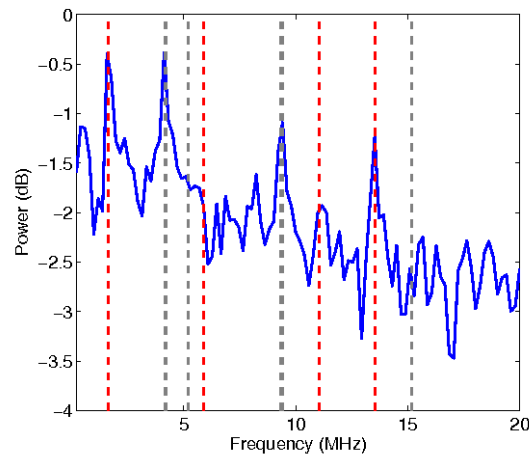
All observed events map into one of five patterns of breakdown noted above where the FT peaks of the data match those of the predictions if the isolated cells have essentially equal fields initially. The fact that all possible iris patterns are seen during the experiment supports the assumption that the breakdowns do not significantly detune the neighboring cells. Hence, the peak probe spectra provide a unique signature that is likely indicating the iris on which the breakdown occurred.



(a)



(b)



(c)

Figure 4: (a) The blue and red dashed lines are the probe power and reflected power, respectively, when the cavity discharges at the end of the pulse (no breakdown), and the solid lines are these waveforms for a breakdown event where the time scale has been shifted so $t = 0$ aligns with the beginning of the normal discharge. (b) The FT of the log of the probe power in the 0-12 μs time range (blue solid line), and the peak spectral frequencies in the simulated measurement in the case where the first

iris is blocked. (c) Same as (b) but for the 12-18 μs data, and the case where no irises are blocked in the simulation but only the downstream four cells are filled initially.

SUMMARY

The 5-cell, 1.3 GHz cavity has met the gradient goals for the ILC positron capture accelerator although the breakdown rate of 1/hr is about 10 times higher than desired. Based on the breakdown rate dependence on gradient observed in other cavities, the rate at 12 MV/m should be acceptable. The cavity will continue to be run to see if the breakdown rate continues to decrease as it has in X-band structures, and to measure the breakdown rate dependence on gradient and pulse width.

The cavity has also provided useful test bed to explore breakdown phenomena. To aid this study, an equivalent circuit was established that was shown to match well particular static and transient properties of the cavity under normal operation. For the breakdown events, it was assumed that the cavity is isolated at a given iris and the stored energy is then partitioned into the modes for the reduced number of cells. The peaks in the probe power spectrum from breakdown events match well the patterns predicted by this model. Thus, such a comparison appears to provide a means of localizing the breakdowns, which is generally hard to do in SW cavities. If more probes could be added to the cavities (e.g., one in each cell), perhaps the details of the plasma evolution could be measured.

ACKNOWLEDGEMENTS

We wish to thank Juwen Wang, Zenghai Li, Chris Nantista, Erik Jongewaard, Gordon Bowden and the Test Facilities Group for their efforts on the design, construction, cold testing and high power operation of this cavity.

REFERENCES

- [1] J.W. Wang et al., 'Studies of Room Temperature Accelerator Structures for the ILC Positron Source,' SLAC-PUB-11767, May 2005.
- [2] J.W. Wang et al., 'Positron Injector Accelerator and RF System for the ILC,' SLAC-PUB-12412, March 2007.
- [3] F. Wang, C. Adolphsen, and J. Wang, 'Performance of a 1.3 GHz Normal-Conducting 5-Cell Standing-Wave Cavity,' SLAC-PUB-13459, Nov 2008.
- [4] M. Johnson et al., 'Arrival Time Measurements of Ions Accompanying RF Breakdown,' NIM A 595 568-571, 2008.
- [5] Chris Adolphsen, private communication.